International Journal of Physical Education and Sports
ISSN: 2411-7242, Volume 2, Issue 2, August 2016

Image Registration of Differential Equations Based on the Calculation of the Score of Sports Events

Shuaili WANG
Modern Education Technology Center, Hunan City University, Yiyang, Hunan, 413000, CHINA

Abstract: Because the traditional partial differential exist image blur, information read errors and large error defects, this thesis proposes the image registration of differential equations. This theory is based on differential equations to classify different classification, to build the model for different types for differential equations based on the application of image registration, and finally to take simulation experiments for different application of differential equations according to different images. Simulation results show that: the model of partial differential equations in this paper is easier to extract and recognize image information extraction, so it is good for reading, but also more clearly and accurately to achieve an effective registration.

Keywords: Image feature; Evolution; Penalty function; Gradient modulus

1. Introduction

Image segmentation and image registration are the two main basic tasks in image processing; they are important parts of machine vision, pattern recognition, and other areas. Registration and image segmentation exist from image arising, many researchers have proposed a lot of treatment, but because of the complex content of the image, and user needs vary, each method is often only applicable to a particular image or demand, making these two issues are still research hotspots in the image project [1]. In addition, Yezzi proposed registration and segmentation mixture model based on those linkages between registration and segmentation [2]. Mixture method has also become a hot issue in recent image processing. Partial differential equation, stochastic modeling and wavelet constitute a theoretical basis for image processing, compared to the other two models , the theory of partial differential equations has the following outstanding advantages: a) has a strong scalability, a variety of image processing theory can be well integrated under the theoretical framework of the partial differential equations; b) can be closely connected with multi-scale analysis and provide an efficient algorithm for a variety of image processing problems; c) has a good theoretical support, applied mathematics, differential geometry and other aspects of the theory results provide mature theoretical basis for new method [3-9]. The research based on image segmentation of partial differential equation and image registration methods has lasts for a long time and it is fruitful. Image segmentation method based on active contour model and image registration method based on optical flow field and other physical models are typical. This paper based on theory of partial differential equations, talking about specific issues in image segmentation and image registration, presents an improved method and effective solutions.

Partial differential equations based on image processing techniques originated in the earliest research on image smoothing and image enhancement by NagaoRudi, and the development milestones has to be attributed to Witkin and Koenderink which introduce the scale-space concep to partial differential equations. Koenderink and Within note that the multi-scale of image obtained by Gaussian filter is equivalent to isotropic diffusion heat conduction equation, according to this theory, researches based on partial differential equations has opened a new chapter. Image processing based on partial differential equations includes image reconstruction, image segmentation, medical image processing and image edge extraction.

2. Partial Differential Equations

2.1. Theory of partial differential equations

Image processing algorithms of partial differential equations inevitably have some drawbacks, including large amount of computation, manual handle needed to adjust the parameters. Based on its advantages of local self-adaptive, normative, and flexibility partial differential equations are widely used in the field of image processing, including segmentation, enhancement, registration, fusion and de-noising method. Image processing model based on partial differential equations can be divided into three categories: (1) the anisotropic diffusion equation method. The most famous equation is P-M equation, which is mainly based on partial differential equa-

tion model to deal with issues and experience purpose, determining the direction of diffusion and diffusion partial differential equations. (2) Model based on energy pan function, which is mainly through establishing the energy functional and seeking extremes to achieve the goals. (3) Geometric describing method, this method is mainly for modeling the evolution of curves and surfaces in image.

2.2. Heat partial differential equation

Thermal diffusion equation was first introduced image processing for image denoising problem solving, and gradually formed a class of diffusion theory of partial differential equations based image processing method. In the field of partial differential equations it has a very important position, which is described in a particular area. The variation of temperature with time "Assuming heat conduction spread evenly in three-dimensional media such as the direction, then the heat conduction equation is as following:

$$\Delta^2 = \frac{\partial^2}{\partial l^2} + \frac{\partial^2}{\partial j^2}$$

Wherein, $\frac{\partial^2}{\partial l^2} + \frac{\partial^2}{\partial j^2}$ is temperature, which is the function of time variable t and space-variable (l, j); $b(a,b)r$ is the thermal conductivity function and function f is already known. If the media considered is not the entire space, in order to obtain a unique solution of the equation, u must be specified as the boundary conditions. If the medium is considered as the entire space, in order to get the unique, the growth rate of solutions must be assumed to have exponential upper bound.

Just like Gaussian function, solution of heat equation corresponds to the initial image as a Gaussian low pass filter, thus preserving the low frequency components of the thermal diffusivity of the initial image, to filter out high frequency component and the high frequency component including details and noise. "Because the heat equation is an isotropic, it is the diffusion equation. Although the heat equation is able to remove the noise but not well protected edges.

2.3. Partial differential wave equation

Wave equation is common and important partial differential equations. It has been showed many times in different areas, such as fluid dynamics, electromagnetics and acoustics. Usually we use the wave equation to expresse all kinds of waves, such as light waves, sound waves and other kinds of waves. The general form of the wave equation is as follows:

$$\begin{cases} \lambda\Delta^2 a - w_j\left(w_j a + w_l b + w_r\right) = 0 \\ \lambda\Delta^2 v - w_j\left(w_j a + w_l v + w_r\right) = 0 \end{cases}$$

3. Partial Differential Value Calculation

There are several methods for solving partial differential equations, and the most common methods including finite difference method, finite element method, finite volume method and finite difference method. Although the procedure is simple and less calculation, the applicability is poor. The method of this idea is mainly by using a differential equation to solved approach to solve differential equations, finite element method, while applicability. But the program is complex, and there are large amount of calculation and finite volume method. So in the image field, for PDE equation, finite difference method is generally used to solve this problem. Commonly used differential forms including:

First-order forward difference:

$$Mean = \frac{\sum_{j=1}^{m}\sum_{j-1}^{m}\left(w_1(j,l)\right) - w_2(j,l)}{m \times n}$$

Second-order backward difference:

4. PDE-based Self-adaption Anisotropy Registration Model

4.1. Image registration model of partial differential

Image registration and segmentation are two basic tasks in the project, and has been researched separately as two separate problems for a long time, Bansal, Yezzi and other researchers noted that the registration process and image segmentation process can utilize each other and promote, and proposed coupled model which combined registration and segmentation. The basic idea is: to take full advantage of the two images on the evolution curve shape similarity to achieve mutual promotion registration and segmentation, which is shown in Figure 1. On one hand, the similarity of target curve shapes on two images promote the changes of displacement field; on the other hand, action on the evolution curve in reference map through displacement field to facilitate the evolution of the curve in the Figure 1.

Figure 1. Registration divides heterosexual registration model

Differential optical flow field basic model is constituted by data item and regular item, the improvements of this article include: structure anisotropic regularization term

in order to maintain the discontinuity of the image, protect the information on the edge of the image, and use of non-quadratic penalty function to enhance the strength of the model.

Noise problem is an important issue in image processing, although do Gaussian convolution towards data item can eliminate noise, but it will also cause image blur, in order to let the data item be able to protect the edges of the image while de-noising, this paper constraints the data item of two sub-type form, it means data item is defined as non-quadratic penalty function of constant constraint, and requires the penalty function has the ability to accelerate the smooth of continuous area, and the smooth of heterogeneous discontinuous region, therefore, this article a select nonlinear total variation model which has good well-posedness.

The above penalty function operate on data item, we can get the following data item of non-second penalty form

$$L_n = b_0 + b_1(t_i - t_0) + a_2(t_i - t_0)^2 + \Delta(i = 1, 2, ..., n) \quad (1)$$

4.2. Self-adaption anisotropy regular term

Horn model uses the Laplace operator as regular term, and Laplace operator can be decomposed into the diffusion of tangential direction and the normal direction according to local structure of the image.

In it, t_{ee} and t_{mm} respectively represent the second derivative along with the normal direction and tangential direction

$$l^{(0)}(m) = (1 - r^0)\left[l^{(0)} - \frac{m}{n}\right]e^{-a(r-1)} \ m \succ 1 \quad (2)$$

In fact, the weighted sum Laplace operator which can be decomposed into tangential and normal direction is the most classical diffusion operator. Therefore the regularization term of differential model is rewriting as

$$\hat{a} = \left[\hat{a}\ \hat{u}\right]t \quad (3)$$

Wherein, α represents the size of the amount of diffusion along tangential direction; β represents the size of the amount of diffusion along normal direction. Obviously, the diffusion process is determined by the coefficient, so the structure of the regular item which has specific spread function, attributed to determine the problem about the size of α, β. In order to keep the edges of the image during the evolution process, the image evolution should maintain the diffusion of tangential direction, and inhibit the diffusion of normal direction; besides, during the registration process, consider protecting the corners not being diffused. Since the target sharp corner has a large gradient and curvature, and the character of target edge is large gradient, small curvature; while the noise location has large curvature, small gradient, gradient in smooth area is small, and the curvature is small, so α, β definition can take values as follows:

$$A = \begin{bmatrix} -\frac{1}{2}\left[l^{(1)}(1) + l^{(1)}(2)\right] & 1 \\ -\frac{1}{2}\left[l^{(1)}(2) + l^{(1)}(3)\right] & 1 \\ \vdots & \vdots \\ -\frac{1}{2}\left[l^{(1)}(n-1) + l^{(1)}(n)\right] & 1 \end{bmatrix}, L\begin{bmatrix} l^{(0)}(2) \\ l^{(0)}(3) \\ \vdots \\ l^{(0)}(n) \end{bmatrix} \quad (4)$$

4.3. Contour model of partial differential

The most representative parametric active contour model is the snake model proposed by Kass et al I30]. The definition of the model is in a nearby region of interest with energy by minimizing the energy function to fit the image data, and the minimum of energy is to make the inside and outside curves and reaches a minimum weighted energy, wherein the internal energy of the curve described tension and smooth power. The external energy is determined by the image information, object boundary energy curve reaches a minimum, the model definition, spline curve $\hat{a} = (b^t b)^{-1} b^t l$ represents point vector in-Snake control; curve $[x_1, x_2, ...x_n]^f$ control the internal energy and external energy, so the curve energy $[y_1, y_2, ..._n]^f$ is composited by the outside curve $[y_1, y_2, ..._n]^f$, namely:

$$X = [x_1, x_2, ...x_n]^f, y = [y_1, y_2, ..._n]^f \quad (5)$$

Wherein, the internal energy $[x_1, x_2, ...x_n]^f$ holding spline elasticity and smoothness, and the external energy $[x_1, x_2, ...x_n]^f$ is determined by the image information, which constraint shows the evolution curve, so that it stops at the boundary of the target. The two energies are defined as follows:

$$y_i = i\left[\sum_{x=1}^{m} \kappa_i, f_1, f_2(net_j)\right] i = 1, 2, ...n$$

Wherein, a and i is the weight coefficient; $i = 1, 2, ...n$ and $i\left[\sum_{x=1}^{m} \kappa_i, f_1, f_2(net_j)\right]$ is the variance of the Gaussian function, $i\left[\sum_{x=1}^{m} \kappa_i, f_1, f_2(net_j)\right]$ is the gradient operator; $i = 1, 2, ...n$ and i respectively corresponding to the first order and second-order derivative of function of $i\left[\sum_{x=1}^{m} \kappa_i, f_1, f_2(net_j)\right]$. The energy functional minimization can be achieved by using differential, FEM, optimization and other methods. Snake model has been proven to be an efficient method to detect the outline, but there is

some problems when the model is used for image segmentation:

(l) The initial contour is required to placed near at the boundary region, and the segmentation results are generally related to the position and shape of the initial contour; (2) non-topological variability is difficult in the recessed area divided image; (3) curve evolution is easy to converge to local minima or isolated at the edge, so to solve these problems, many scholars improved this model according to these short comings. Cohen join balloon force model, and by expanding the scope of the border to avoid looking into local energy pole value; Xu put forward a gradient vector flow snake model. this model of the image gradient field is approximate, and a new force constructed to achieve the division of the recessed area, but the complexity of this method is very high; Menet et al proposed the model B when discussing the snake model for the optimization process, especially for the problem of the first-order profile and two order derivative not be obtained accurately data; While A nit proposed dynamic programming algorithm to solve global optimal curve snake, numerical stability of the method, which could also exist the problem of high computational complexity.

D. Self-adaption Anisotropic Registration and Solution Based on Partial Differential Equations

In the differential optical flow field model, the adaptive penalty function can be set in the amount of optical flow model. In order to enhance the ability and Robusting of its model, the formula take data items (7) into the partial differential equation (8) to obtain the best energy pan function expression as follows:

$$net_j = \sum_{x=1}^{m} \kappa_i, f_1, f_2(net_j) = f\left(\frac{net_j - b_j}{y_j}\right) \qquad (6)$$

first provide initial velocity field (u_0 , v_0), here set the initial velocity field as 0, then do iterative solution, in each iteration, the solution for velocity field are calculated through the velocity field obtained from previous iteration calculation, the specific expression is

$$u_j = \begin{cases} \frac{3-\sqrt{3}}{9} & \frac{\sqrt{3}-1}{3} & \frac{3-\sqrt{3}}{9} \\ -\frac{3-\sqrt{3}}{9} & -\frac{\sqrt{3}-1}{3} & -\frac{3-\sqrt{3}}{9} \end{cases} \quad u_l \begin{cases} \frac{3-\sqrt{3}}{9} & 0 & \frac{2-\sqrt{3}}{9} \\ \frac{\sqrt{3}-1}{3} & 0 & \frac{2-\sqrt{3}}{9} \\ \frac{3-\sqrt{3}}{9} & 0 & -\frac{\sqrt{3}-1}{3} \end{cases} \qquad (7)$$

Here, k is the iteration number, $w \in [0,2]$ is the relaxation coefficient, h is the step size. In formula (20), ∂ , β use formula (9) to get the solution; a_{ee} , a_{mm} , v_{mm} , v_{ee} are the most advanced differential operator, they can use formula (10) and the formula (11) to achieve, for numerical stability, LUCIDO L proposed to use adaptive template to calculate a_{ee} which shows in Figure 1.

For first derivative u_j and u_l , this paper adopt the template which is similar to Sobel gradient operator to calculate, there is a certain kind of noise immunity in this template, which is able to estimate the value of image gradient better

$$\partial a_{ee}(l, j) = -5\lambda_0 u(l, j) + \lambda_1 \left(u(l, j-1)\right) \qquad (8)$$

As v_{ee} is the same as u_{ee} , both of them need solution of speed on tangential direction, so solving method is the same; on the other hand, u_{ee} and v_{ee} have similarities in the expression form, the numerical calculating method for u_{ee} only need to change u_j and u_l in the template for calculating UTT to u_j and u_l respectively; solving v_{ee} is similar with u_{ee} .

5. Experimental Simulation and Analysis

5.1. Registration evaluation

The following experiment is for single-mode and multimodal brain MR images, all experimental parameters take " $\beta = 0.03$, $\eta = 3.5$, " $r = 0.3$, the time step $w_1 = 0.3$, the basis of iteration termination judgment takes the maximum amount of displacement which is no more than 0.01. In each figure, contour curve is red. In addition, we compared the present model and representative Wang model. Quantitative analysis of segmentation result commonly uses Js. and De to measure; registration results use the average gray difference, MSE and mutual information for evaluation.

In this paper, we introduce edge-aligned degrees based on these three common evaluation parameters, in order to better detect the registration results about the edges of image.

A) Mean Intensity Subtraction

$$a(l, j, r) = \frac{el}{er} = \frac{\Delta l}{\Delta r}, b(l, j, r) = \frac{dj}{dr} = \frac{\triangle l}{\Delta r} \qquad (9)$$

In it, *Var* is the mean square error, if the Peak signal to noise ratio is larger, the better.

Alignment Metric of Edge. The concept of alignment metric is from the understanding of contents of two aligned images from human eyes; from microscopic point of view, this means that each gray level of an image at pixel location corresponding to another image gray level is stable most. The process of solving alignment metric is

$$a(l, j, r) = \frac{el}{er} = \frac{\Delta l}{\Delta r}, b(l, j, r) = \frac{dj}{dr} = \frac{\triangle l}{\Delta r} \qquad (10)$$

In formula (9) to (10), $w_1(j,l)$ represents the image after registration, $w_2(j,l)$ represents the reference image;

$E(1,2)(n)$ and $E(2,1)(n)$ are gray value in two images that one image whose pixel gray level is n corresponding to another image; $h_1(n), h_2(n)$ represents that the number of pixel gray value is n; $p_1(n), p_2(n)$ represent the pixel rate of which the pixel value is n in two images. CW in the range $[0,2]$, use Kuang Yabin's infrared and visible image registration algorithm directly request reciprocal for CI, then get the alignment metric (AM), that is

$$AM = \frac{1}{CI}$$

However, the range of alignment metric is too wide, so alignment metric in this article is:

$$AM' = e^{-CI}$$

Because when registration between two images, the value of alignment metric AM ' is the greatest.

5.2. Optical flow experimental of rubik chart

Rubik Chart is one of the most representative test charts of the optical flow field; first, choose this chart to validate the registration result of the model in this paper. Use Rubik Chart placed at an angle 2 (a) to be chart waiting registration. Rubik Chart rotates in certain angle 2 (b) as a benchmark figure, three models were used 100 times iterations. The results can be seen from Hom model 2 (c), Hom model results in blurred images quickly , as well as the edges of the image is difficult to distinguish; Registration result in Figure 2 (d) of Weickert model shows that the diffusion model defined by Weickert has enhanced ability to maintain the edge of the model, it is better than Hom method, but on the top of Rubik whose working speed is fast (fierce change of the performance of the image), image characteristics can not be effectively maintained and edges severely blurred; registration results of this model (Figure 2 (e)) shows that this model can maintain image features and applies to all forms of image motion, and has better adaptability on fast motion, and the registration accuracy is significantly better than the other two models. The mean and variance of registration results in our model is minimum, which further explains the registration result of our model is the closest to reference image.

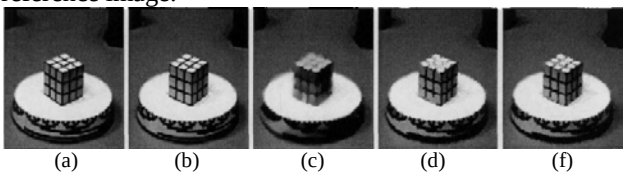

(a) (b) (c) (d) (f)

Figure 2. The diffusion model defined by Weickert has enhanced ability to maintain the edge

5.3. Brain MR image registration

Brain MR Chart is the most representative figure of optical flow field experiment, this experiment choose two brain MR images to be an image waiting registration and the reference image, in the case of constant illumination, choose Horn model and Lucas-Kanade model for comparative experiment. Horn model and model of this paper do iteration for 30 times respectively, window size of Lucas-Kanade model is 5, 5 layers iteration deformation between two images, and optical flow vectors shown in Figure 1, and then get the registration image which is shown in Figure 3. Figure 3 (e) shows the enlarged partial ventricle area in each image, you can see the registration and segmentation results more clearly of each model. The parameter value in table 3 further illustrates the effectiveness of our model to deal with complex images.

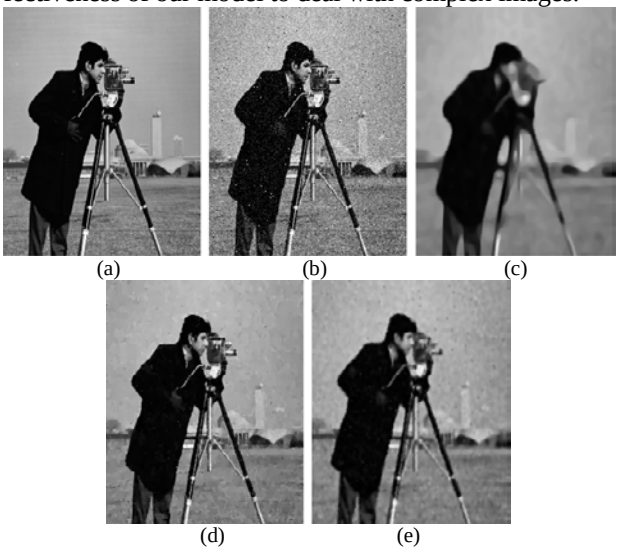

(a) (b) (c)

(d) (e)

Figure 3. Registration of brain MR image

From the experimental results Figure 2 (c), we can see Horn model lead to image blurred quickly, and image edges and corners severely blurred and difficult to distinguish. Figure 2 (d) shows the registration results of Lucas-Kanade model, the upper edge of the image appears error message, verify that the model select window registration make image edge information loss, but the registration for the target image is superior than Horn model. The registration results of model presented in this paper (Figure 2 (e)) shows that this model is able to maintain image features, good attention to detail, and the closest to the reference image.

5.4. Different pictures of multi-modal human brain

The experiment realizes the registration of brain MR images of T1, T2 two modals and the segmentation of upper ventricles organization. Treat the clearer organization T1 picture as basic map (Figure 4(a)), and treat the fuzzy picture T2 to be segmented, the initial reference curve uses a known figure ventricle contour curve, as shown in 4 (b). Our model and the Wang model can

overcome brightness inconsistencies, which can achieve the valid registration from T1 to TZ.

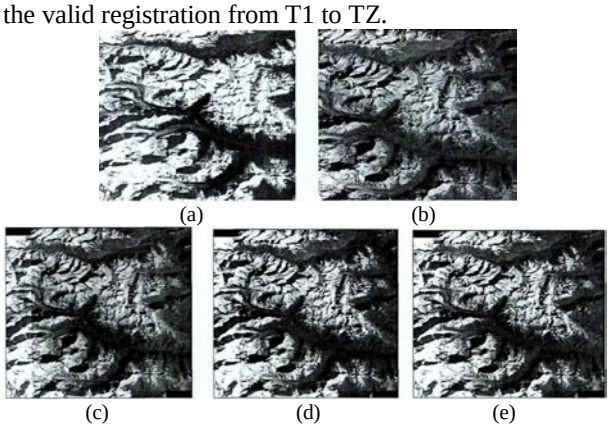

Figure 4. Experiment Result of Multi-modal Brain Figure MR

The data in Table 1 adequately describes the registration result of our model is significantly better than the Horn model and the Lucas-Kanade model, and is closest to the reference image, the peak signal to noise ratio is also the largest, indicating that this model has better strength. In addition, because Horn model is fuzzy seriously, especially the edge of error is too large, resulting alignment metric is very small; while Lucas-Kanade model appears false information on edge position which cause the alignment metric is small as well; our model has the characteristic of self-adaptive anisotropic, so it protect edges on the registration process avoid being lost.

Table 1. Results evaluation of brain MR image registration

Model	*PSNR*	*Mean*	*Var*
Horn model	34.02	-0.12	31.24
Lucas-Kanade model	32.34	1.62	38.65
Proposed model	38.87	-009	9.23

Table 2 shows for brain MR images, this algorithm with other algorithms comparison of computing time. As can be seen by comparing, the computation time of this proposed algorithm is longer than the Horn model, than Lucas-Kanade model runs a short time. Mainly due to: 1) This article is a Horn model improvement in the data items and regular items on the design than the Horn model complexity; 2) Lu-cas-Kanade model is a hierarchical sub-window iteration, the window is smaller, the more stratified and more complex the model which is the Lucas-Kanade one of the drawbacks. As can be seen from Table 3, this model greatly improved the accuracy, computing time and did not slow down too much, indicating that the algorithm is effective.

Table 2. Computing time comparing among our algorithm with other algorithms

Model	Image Size	Iterations	Computation time/s
Horn model	260*220	32	1.40031
Lucas-Kanade model	260*220	Size of window is 5.6 layer iteration	3.80625
Proposed model	260*220	32	1.56051

Since the differential optical flow field model constructs regularization term starting from a smoothness constraint, so the evolution of image will inevitably result in blurring, the registration process is a process of iterations, therefore, the image with increasing number of iterations becomes smooth is an inevitable trend, results also reflect this phenomenon, Hom method is simple, fast, but can cause severe image blur; use edge enhanced model of WIckert on image registration, although able to keep an edge better than Hom model, but because the model is proposed for static noise images, so that the model can not achieve accurate registration on the part which change violently. The model in this paper uses anisotropic diffusion as a flow-driven regularization term, according to the local image structures to control the evolution of the image, the character of the image can be maintained well; data item uses non-quadratic penalty function which effects on the brightness constant assumption, and make the model suitable for brightness changes caused by various motion, and it is more robust.

5.5. Registration of human face images

To validate our model is suitable for image with illumination changes, this experiment choose two face images for registration. Observe from figure 5 , in Figure 6 illumination changed significantly, all three models were used 20 iterations, the obtained vector of optical flow field is shown in Figure 6. Experimental results show that both the whole or partial view, Horn model seriously obscure the image, so that we can not recognize (see Figure 5 (c)), once again validate the limitation of the Horn model; the registration result of Lucas-Kanade model obviously loss the moving edges; our model has better retention ability to image detail, and the illumination image can be changed to achieve more satisfactory results, the data in Table 4 further illustrate the registration result of this is the closest to the reference chart.

Figure 5. Registration of face image

Figure 5 Result: The division result comparison of four methods on artificial image, line 1: the original image and the initialization curve; Line 2: segmentation of Contrast constraint LBF model; line 3: division result of the

original LBF model: Line 4: segmentation result of PS model.

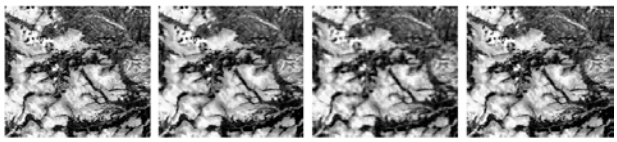

(a) (b) (c) (d)

Figure 6. Optical flow vector field of face image

Table 3. Evaluation for registration results of face image

Model	*PSNR*	*Mean*	*Var*
Horn model	34.03	-4.17	35.25
Lucas-Kanade model	32.36	10.62	38.68
Proposed model	38.89	1.24	9.25

Table 4 shows the comparison of the running time from our algorithm and other algorithms in the experiment of face image. The above results show this improvement is valid.

Table 4. Computation time compared with our algorithm and other algorithms

Model	Image Size	Iterations	Computation time/s
Horn model	200*200	30	1.50031
Lucas-Kanade model	200*200	Size of window is 5.6 layer iteration	7.80624
Proposed model	200*200	30	2.86041

6. Conclusion

With the continuous development of the partial differential equations theory and application, different image distribution of partial differential equations has become hot spots nowadays. This article is based on defectives of the optical flow image processing motion pull bits, like large errors, not clear image, vague and so on. Based on the partial differential adaptation, heterosexual image standard model is proposed and researched. So through the classification of partial differential equations models and applications of equation theories, the simulation experiments for different images' have been carried out, and the results show that when using the partial differential equations of the adaptive image, its image resolution has been significantly improved, reading take enough fast and accurate, which effective protect the tangential direction and inhibit diffusion directions, and successfully protected the edges and corners of the image.

References

[1] Muhammad J. Mirza, Nadeem Anjum. Association of Moving Objects Across Visual Sensor Networks. Journal of Multimedia, Vol 7, No 1 (2012) pp. 2-8

[2] Ying Yang, Xin Gao. Remote Sensing Image Registration via Active Contour Model. International Journal of Electronics and Communications, 2009,63(4):227-234

[3] Qiu Yina, Li Junli, Wei Ping, Jin Linpeng, Jin Wei. A Medical Image Registration Method Based on Gravity Optimization. 2009 3rd International Conference on Bioinformatics and Biomedical Engineering (ICBBE), 2009,1-4

[4] Zhang Jingzhou,Huo Pengfei,Teng Jionghua. Multi-resolution medical image registration based on generalized mutual information. 2010 3rd International Congress on Image and Signal Processing (CISP), 2010, 3:1244-1247

[5] C. Schmid, R. Mohr, C. Bauckhage. Evaluation of interest point detectors. International Journal of Computer Vision, 2000, 37(2):151-172

[6] Gouet V, Montesinos P, Deriche R, et al. Evaluation de Detecteurs De Points Dint Eret Pour la Couleur. Reconnaissance des Formes et Intelligence Artificielle (RFIA'2000), Paris, 2000:257-266

[7] Shen Mei-li. An Effective Target Tracking Method. Second International Symposium on Electronic Commerce and Security(ISECS 09),2009,1:499-502

[8] Guo Chenguang, Li Xianglong,Zhong Linfeng,Luo Xiang. A Fast and Accurate Corner Detector Based on Harris Algorithm. Third International Symposium on Intelligent Information Technology Application (IITA), 2009,2:49-52

[9] Zhang Jinping, Lian Yongxiang, Jiao Chunwang, Guo Dameng, Liu Jie. An improved Harris corner distraction method based on B_spline. The 2nd IEEE International Conference on Information Management and Engineering (ICIME), 2010:504-506